

## Biomimetics in Ship Design?

Blanca Pena<sup>a</sup>, Ema Muk-Pavic<sup>a</sup>

*Department of Mechanical Engineering, UCL, London, WC1E 7JE, UK*

---

### Abstract

The hydrodynamic performance of ships can be improved by the retrofit of Energy Saving Devices (ESDs). These devices are typically seen in the aft part of the ship hull and act by lowering the ship resistance, conditioning the fluid in front of the propeller and/or recovering energy from the rotational swirl of the fluid leaving the propeller.

Technological gaps in the field suggested that there is a room for the development of a new biomimetic ESD based on ‘tubercles’ technology. Tubercles are rounded structures naturally found on the leading edge of the Humpback’s whale flipper and they are capable to hydrodynamically control the flow around the whale. Similarly, a novel device has been created to control the flow around the aft part of the hull, reducing ship’s resistance and improving the wake conditions in which the propeller operates.

This research paper presents tubercles technology, working principles and the results from the first numerical experiments of a full-scale ship fitted with the created tubercled ESD. The results from this investigation revealed a promising potential of this novel technology.

*Keywords:* hydrodynamics; ESD; biomimetic; tubercles; full-scale; ship efficiency

---

### 1. Introduction

In the shipping industry, greenhouse gas emission is already subject to the International Maritime Organization (IMO) regulation. The existing criteria and the one coming into force are stringent.

In order to enhance ship efficiency, all possible improvements are required. Among them, fuel cells, air lubrication systems, the use of natural resources such as wind, solar energy and magnus effect cylinders can be found on the market. These devices are promising; however, ones of the most inexpensive and convenient are the hydrodynamic aft Energy Saving Devices (ESDs), (DNV GL, 2016, Hemmera Envirochem Inc, 2016).

ESDs are present as appendix structures and/or modifications to the propeller, hull or rudder with the primary goal of improving efficiency and reducing the fuel consumption of the ship. They are typically seen in the aft part of the ship hull and act by lowering the ship resistance, conditioning the fluid in front of the propeller and/or recovering energy from the rotational swirl of the fluid leaving the propeller.

Based on their position on a ship, ESDs are classified in three different zones: Zone I before the propeller, Zone II in the propeller region and Zone III downstream of the propeller (Carlton, 2012). These zones are shown in the Fig. 1:

---

\* Corresponding author *E-mail address:* blanca.pena.16@ucl.ac.uk

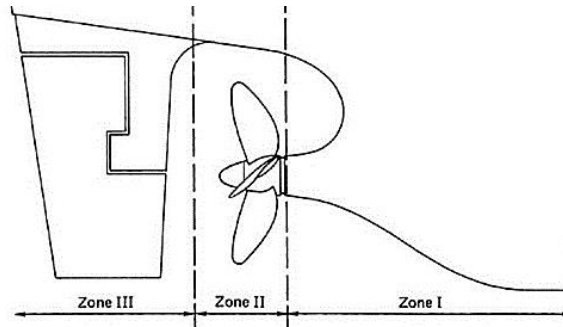


Fig. 1. ESD Classification Zones (Carlton, 2012).

The devices in **Zone I** or Pre-Swirl devices are located upstream of the propeller. They aim to modify the flow that enters the propeller, manipulating the aft ship's boundary layer or pre-swirling the flow (Carlton, 2012). The output is a more homogenized velocity distribution in the wake field (Molland, 2011), or a reduction of the rotational swirl in the downstream propeller fluid. Examples of these are the Wake Equalizing Duct, Mewis Ducts, fins such as Vortex Generators or Grothues Spoilers (Carlton, 2012).

**Zone II** devices operate directly at the propeller. Many examples include the modification of the propeller blades or the attachment of free rotating mechanisms that use the remaining kinetic energy in the propeller slipstream. Non-conventional propellers are included among these devices. An example is Contracted and Loaded Tip (CLT) propeller that have demonstrated a 6-12% reduction in fuel consumption in more than 300 commercial vessels (Gougoulidis & Vasileiadis, 2010).

**Zone III** or Post-Swirl devices are typically located behind the propeller and they take advantage of the kinetic energy found within the rotational swirl of the slipstream. From that kinetic energy, they generate additional thrust. Grim Vane Wheel is an example of free rotating devices that act as an extension of the propeller, generating additional thrust (Carlton, 2012).

From the extensive literature review conducted by the authors, it has been found that there is an opportunity for the development of an energy saving device based on an ancient biomimetic technology. Our inspiration came from the superior hydrodynamic performance of certain aquatic mammals (whales) that operate in similar flow regimes that a ship does. Our aim is 'to mimic' their unique geometry into an ESD solution, with the aim of controlling and manipulating as desired the flow around the hull. The ancestral flow control technique that certain whales use to achieve high speed and turns is based on 'tubercles'. Until today, there is no evidence that tubercles have ever been applied in hull geometries with the aim of improving the overall ship hydrodynamic performance.

This paper presents a comprehensive review on tubercles technology, the state of the art and challenges. Tubercles mechanisms of action in turbulent regime (a normal full-scale ship regime) are also reviewed. Based on the mechanisms of action in turbulent flow regime together with the hydrodynamics of a hull, it was possible to identify and quantify the improvements needed and design a novel biomimetic energy saving technology that achieves the desired effect for purpose. Finally, the designed tubercled ESD is numerically tested in a full-scale ship and its impact on resistance and nominal wake field quantified.

## 2. Tubercles

Tubercles, or lumps in the leading edge of a foil are sinusoidal rounded structures naturally found in Humpback Whale's leading-edge flippers (Fig. 2). The most important parameters that define a tubercled sinusoidal geometry are the amplitude 'A' and wavelength ' $\lambda$ ', defining the locations of the peaks and troughs (Fig. 3) along the leading edge



Fig. 2. Humpback Whale (Wikipedia, 2019)

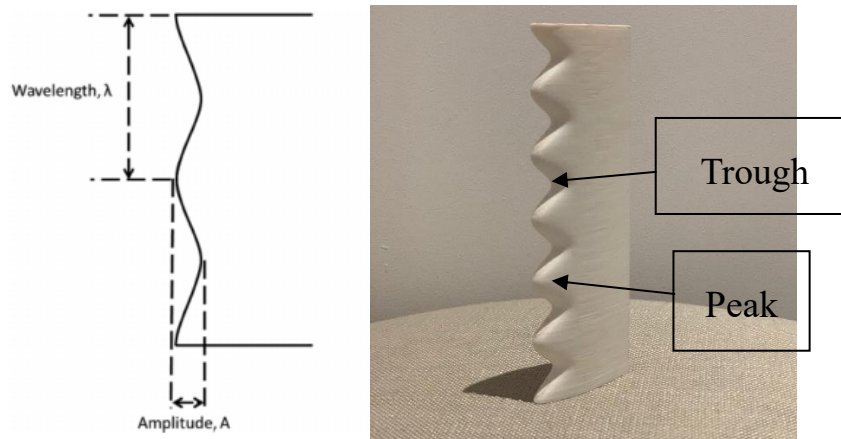


Fig. 3. Tubercles main parameter representation (Left) (Hansen et al, 2009) and isometric view of authors 3D printed tubercled foil (Right)

### 2.1. Tubercle Effect

Tubercles in whale flippers were first time technically described as lift enhancement devices in 1995 (F. E. Fish & Battle, 1995), recognising that tubercles can delay stall and increase the maximum lift coefficient of the flipper.

The first numerical analysis of leading edge tubercled wings was conducted by Watts and Fish (2001). This analysis reported that at 10deg Angle of Attack (AoA), tubercles caused an increase in lift and a reduction of the produced drag. Fish et al, (2006) conducted RANS simulations of the NACA 63021 baseline foils (smooth foil) and modified (leading edge tubercled foil) at a Reynolds Number of 106 (transitional near-turbulent regime) with a 10deg angle of attack. From their numerical analysis they concluded that pressure changes dramatically when tubercles are incorporated. Large vortices were seen behind the troughs and separation delay was identified behind the peaks, near the trailing edge.

Miklosovic et al. (Miklosovic, Murray, Howle, & Fish, 2004) experimentally tested three flippers shape with and without tubercles in transitional flow regime. This study confirmed that an increase in the maximum lift and an increase in the stall angle was achieved by introduction of tubercles. It was also found that drag decreased for angles of attack between 11 and 18deg. In addition, Miklosovic et al (Miklosovic, Murray, & Howle, 2007), experimented with full-span rectangular wings and semi-span wings finding different results. He found that a semi wing increases lift and decreases drag when compared to the baseline wing, opposite to what a full span wing does. His study concluded that tubercles may behave differently depending on the wing shape.

Parametric studies varying the amplitude and wave length were conducted by Johari et al. (Johari, Henoch, Custodio, & Levshin, 2007) Fig. 4. They studied the performance of NACA shaped wings for a baseline foil (without tubercles) and with leading edge tubercles.

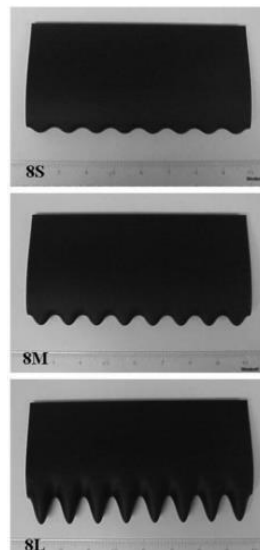


Fig. 4. Johari's tested hydrofoils at different wave amplitudes (Johari et al., 2007).

The results from the experiments (Fig. 5) showed that in the post-stall regime, the tubercles revealed a 50% higher lift than the smooth foil. They also found that the tubercles wave amplitude plays a significant role in the performance of the tubercled foil. Moreover, tufts were attached to the foil surface to observe the separation near the surface and they stated that the flow over the tubercles remained attached well past the angle of attack where the baseline foil stalls.

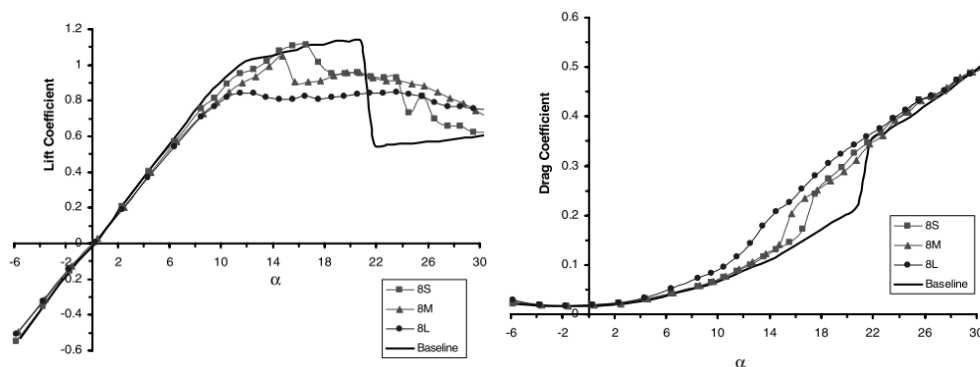


Fig. 5 Leading edge tubercle Johari's experiments (Johari et al., 2007). The legend as on **Error! Reference source not found.**

The investigations conducted in the above listed studies generally agreed on the fact that optimised tubercle profiles could improve the lift coefficient curves further by maintaining the lift after the stall point.

## 2.2. Current Tubercles Applications

Applications of tubercles have looked into the effects of the inclusion of leading edge tubercles in fans, compressors, wind, tidal turbines or rudders, (Shi et al., 2016; Watts & Fish, 2001; Corsini et al, 2013; Swanson & Isaac, 2011). These researchers have stated that the inclusion of tubercles in blades see a delay in the stall and can maintain lift further after stall when compared to a similar baseline (unmodified) blade. This suggests potential applications of tubercles in rotating machinery.

### 3. Tubercles Mechanisms of Action in Turbulent Flow Regime

It is important to remember that at the stern of the ship the flow is turbulent and to date most research has focused on transitional and laminar flow regimes. This fact made difficult to predict how tubercles would behave at high Reynolds numbers and suggested that further research was needed.

An investigation on the hydrodynamics of tubercles in turbulent flow regime was conducted by the authors (Pena et al, 2019) 

The main mechanism of action that characterise tubercles behaviour in turbulent regime is the creation of 3D counter-rotating vortices. These vortices are formed over each tubercle peak and travel in the streamwise direction. The identified vortex structures are formed due to pressure differences that exists between suction and pressure sides of the foil and they are shown in the Fig.6. These vortices work by mixing the upper with lower regions of the boundary layer. This phenomenon is seen at other flow regimes as well (N. Rostamzadeh et al., 2014; Skillen et al., 2014; Skillen et al, 2015).

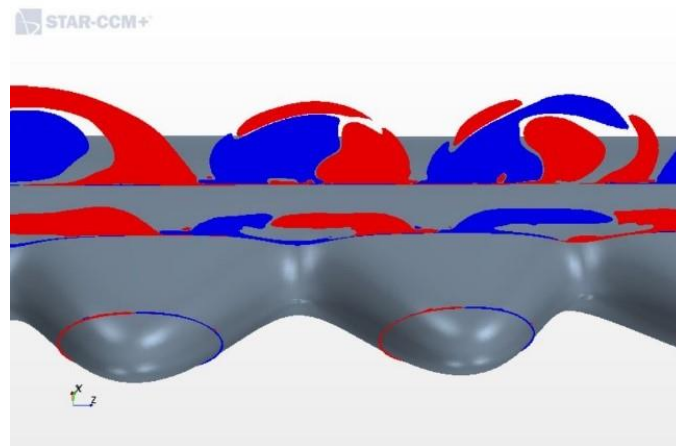


Fig. 6. Evolution of the streamwise vortices. Red represents clockwise vorticity whereas blue represents anti-clockwise vorticity

The secondary mechanism of action present is the existence of a secondary spanwise flow. This is caused by depression areas behind the troughs on the suction side of the hydrofoil. Due to this pressure differences, the flow travels spanwise from the zones of high pressure (peaks) to the zones of low pressure (troughs). This secondary flow is shown in the Fig. 7, where the streamlines are being squeezed towards the troughs. This is consistent with the investigations in a different flow regime (Skillen et al, 2014). Due to this spanwise flow, the low momentum fluid that lies next to the wall is deflected and transported away from the peaks towards the troughs (Skillen et al, 2015).

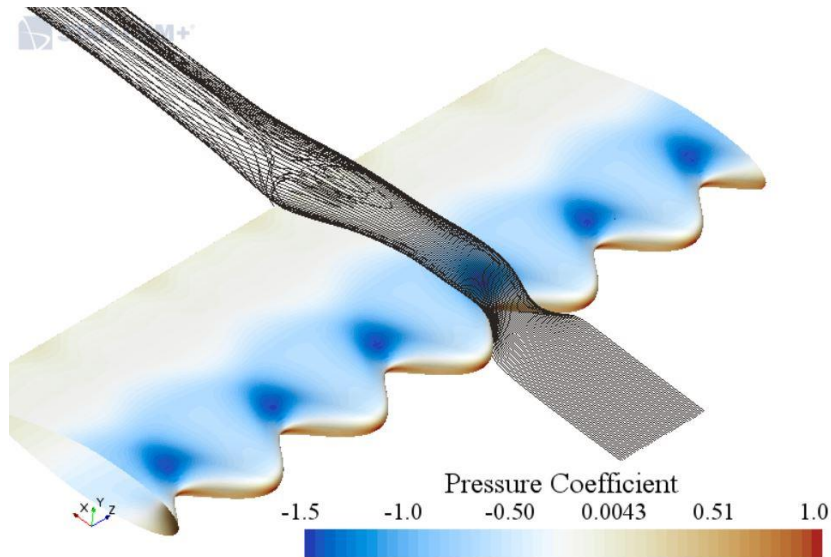


Fig. 7. Pressure coefficient distribution on the suction side of a tubercled hydrofoil together with time-averaged streamlines.

This investigation was essential as it gave us an understanding of the performance of the tubercles in ship flow conditions, granting a full picture of the potentials of tubercles technology as a ship flow control technology.

#### 4. A Novel Tubercled ESD

The novel tubercled ESD is a Zone I ESD, conceived and mounted on the hull with the aim of reducing flow separation, the viscous drag and therefore improving the overall ship hydrodynamic efficiency. This is achieved by tubercles mechanism of action. Tubercles produce a pair of counter-rotating vortices that are introduced to redistribute the streamwise momentum in the ship's boundary layer to better resist an adverse pressure gradient. This counteracts the negative effects of the adverse pressure gradient that is seen on the stern of a hull.

The shape and location of the novel ESD is not revealed yet, however, this paper discloses for the first time the positive effects that the tubercled ESD induces on the hull hydrodynamics. The results showed correspond to the first tubercled device concept design, where the feasibility of the novel ESD is tested.

##### 4.1. Full or Model Scale?

Most of the energy saving devices on the market have been tested and designed in model scale. In most cases, the expecting fuel savings claimed by the manufactures were above what was achieved in the full-scale measured during sea trials.

One of the problems found is that for most of the devices, their measured performance in full-scale was different than predicted based on the model scale investigations in towing tank and CFD. This discrepancy is caused by hull/device interaction that is difficult to accurately predict in model scale as well as due to the known Reynolds number scaling effects that are very difficult to quantify accurately. A flow separation is very pronounced in model scale and vortices encounter higher damping in full-scale. Furthermore, vortices from bilge or struts are much weaker and vanish sometimes altogether in full-scale simulations. Consequently, the wake field in the propeller plane is significantly different at model and full-scale (Fig. 8).

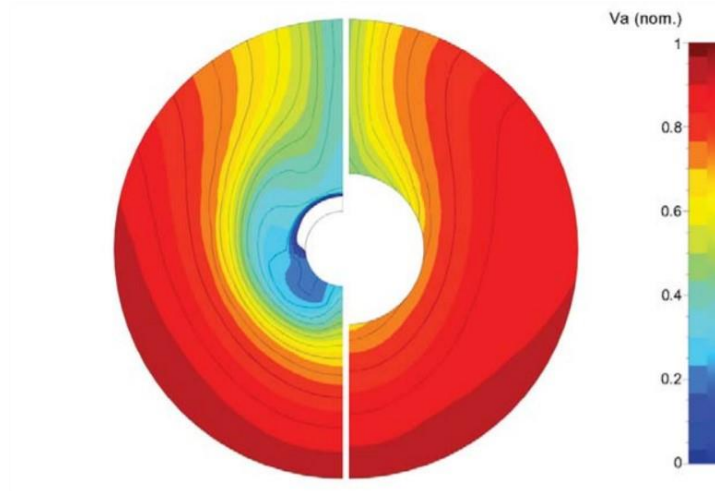


Fig. 8. Nominal wake at model scale (left) and full-scale (right) (Hochkirch & Mallol, 2000)

The changes between model scale and full-scale concern primarily the relatively different boundary layer nature. For that reason, in an effort to avoid issues with scaling, this study directly focuses on the hydrodynamic performance of the ship in full-scale.

#### 4.2. Case Study

The first ESD hydrodynamic performance test is conducted on the full-scale general cargo ship 'Regal'. Regal is a single screw vessel, propelled by a 4 blades propeller with the main particulars summarised in the table below:

Table 1 Regal particulars

Parameter	Units	
Length between perpendiculars	L <sub>pp</sub> , m	138
Breadth moulded	B, m	23
Depth moulded	D, m	12.1
Draught	T, m	Ballast
Propeller diameter	D <sub>p</sub> , m	5.2 (four bladed)
Water Density	P <sub>w</sub> , kg/m <sup>3</sup>	1010
Air Density	P <sub>a</sub> , kg/m <sup>3</sup>	1.1649
Kinematic Viscosity of Water	v <sub>w</sub> , m <sup>2</sup> /s	8.8394 x 10 <sup>-7</sup>

This vessel was selected as it was previously used as a case study for the Ship Scale Hydrodynamics Workshop organised by Lloyds Register (Ponkratov, 2016) and a significant data was available including a full-scale measurements and the 3D full-scale scanned geometry. During the sea trials in a reasonably calm water conditions the speed tests were conducted at ballast draught under three different power conditions Fig. 9. At each shaft speed, power and torque were recorded.



Fig. 9. Sea trials weather conditions (Ponkratov, 2016)

#### 4.3. Scope of Simulation

The problem represents an incompressible viscous flow around a streamlined body, being numerically simulated by a computational fluid dynamics (CFD) code. This study was conducted using the commercial CFD code Siemens Star CCM+, using a transient DES family turbulence model method. The computations are run in an HPC parallel multi node Linux cluster, using 200 simultaneous cores. In average the duration of a single simulation was around 48 hours.

This work consists of three sets of numerical simulations conducted in a full-scale at the ballast condition for three different shaft speeds:

- self-propulsion simulations in a full-scale (including propeller and rudder).
- bare hull simulations with rudder only,
- bare hull simulations with rudder and the novel tubercled ESD

All simulations have been done in clean condition corresponding to the actual sea speed trials.

Self-propulsion simulation was used to compare the calculated torque with the measured one during the sea trials. This comparison is used to judge the quality and accuracy of the CFD setup and assess the impact of propeller action on the flow. As the numerical investigation is done for the ship in a full-scale and the aim was to investigate flow in a high detail with high accuracy, the setup of the simulation was very rigorous and thorough. The transient numerical simulations were run modelling a ship in the full-scale and allowing the hull to sink and trim freely.

Bare hull simulations were used to investigate the flow in the stern region without presence of the propeller (nominal wake) and understand which elements of the ship hull geometry are impacting on the hydrodynamic efficiency. Based on the results from these simulations it was possible to identify and quantify the improvements needed and design a novel biomimetic energy saving technology that will achieve the desired effect for purpose.

Hull simulations with the ESD are conducted to assess the efficiency improvement through retrofit of the tubercled ESD. Simulations with and without the device are run in same flow conditions.

#### 4.4. CFD Set-up

In order to select an appropriate time-step the Courant-Friedrichs-Lewy (CFL) condition was used achieving a mean Courant number of 1. This ensured the unsteady simulations convergence. The time step was reduced when needed in order to achieve adequate convergence of less than  $10^{-5}$  in the residuals.

All simulations used a 2<sup>nd</sup> order spatial and temporal discretisation for all equations and simulation convergence were monitored for residuals, hydrodynamic torque coefficient ( $K_Q$ ) and ship total resistance coefficient ( $C_T$ ).

The prismatic control volume has one length upstream of the ship, two ship lengths behind the ship and one  $L_{pp}$  towards port and starboard side as shown in the Fig. 10 (left). This separation between the ship wall and the tank ensures an undisturbed far field velocity. A Dirichlet condition is imposed on the inlet.

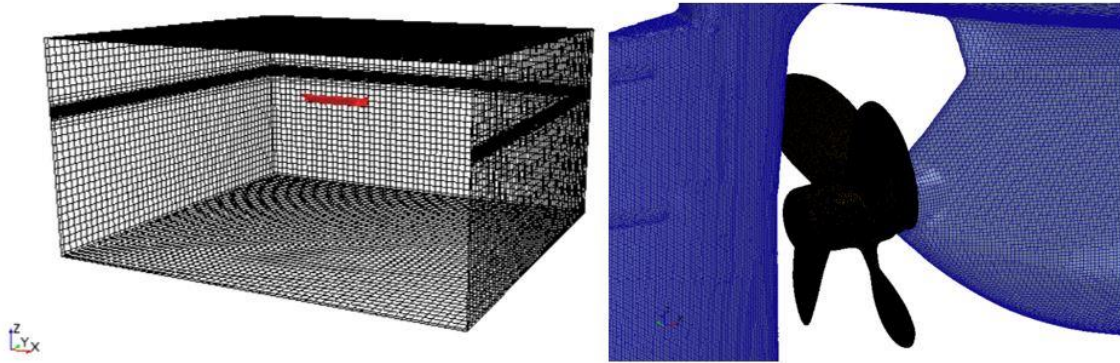


Fig. 10. CFD domain (left) and propeller refinements (right)

Hexahedral (3D) structured cells discretize the volume with local refinements performed at the locations where main flow features are expected. These locations are the rudder, bow and at the free surface.

Significant refinements are conducted at the stern (Fig. 11 left), at device's location (Fig. 11 right) and at the free surface in order to capture flow separation and free surface effects. The Volume of Fluid (VOF) method was used to capture the deformation of the free surface. Second order spatial resolution is used at the free surface. A trimmed mesh was used and was aligned to the still water free surface.

A separate cylindrical domain was created for the propeller to allow for the rigid body rotation to be modelled (Fig. 11 (left)). Internal interface boundary conditions were implemented on the cylinder faces between the rotating and static domains.

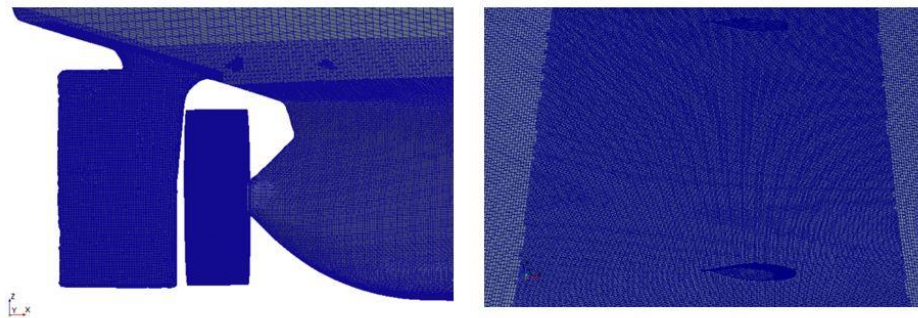


Fig. 11. Mesh refinements on the aft end (left) and on the device's location (seen from inside the hull) (right)

Note that that in the results section the calculation of the nominal wake field is conducted without the propeller. The system of grids used for the towed cases with and without the novel ESD comprises the same validated and verified grids used for the self-propelled case but removing the propeller.

#### 4.5. Validation and Verification

The simulation uncertainty is assessed by using benchmark experimental data for the same geometry self-propulsion test at three different propeller shaft revolution speeds: 71.6, 91.1 and 106.4 rpm. The results for the torque coefficient  $K_Q$  vs the shaft speed (Fig. 12) confirm the accuracy of our setup. This was able to produce results within a 2% difference when compared to the measurements for the torque taken during the sea trials. More details of the validation and verification process for the self-propulsion and bare hull cases can be found in a previous authors publication (Pena et al, 2019).

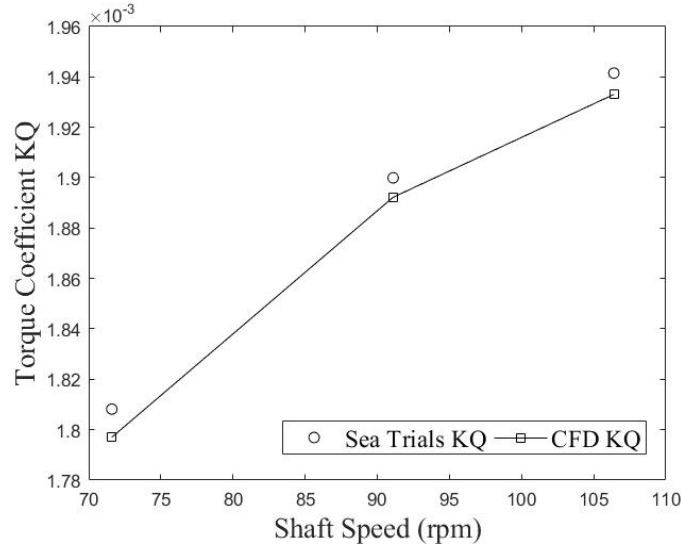


Fig. 12. Validation and Verification of the CFD set-up

For the bare hull simulations with and without the novel ESD, an iterative and parameter convergence study is conducted using 4 mesh resolutions with systematic parameter refinements of the mesh size following the ITTC Quality System Manual Recommended Procedures and Guidelines (2017). Table 2 presents the mesh independency study for the resistance coefficient resulting from the four mesh resolutions for the bare hull setup with and without device. The systematic mesh refinement study is conducted by varying the mesh size input parameter while holding all other parameters constant. The initial uniform parameter refinement ratio is established as  $r = \sqrt{2}$ . As shown in the table, the difference of the calculated ship resistance between grids is called the convergence ratio. This value is a 1.5% between meshes 3 and 4 and therefore no further refinement is deemed necessary.

Table 2 Mesh convergence study

Mesh Name	Million Elements	$C_T$	Convergence Ratio
1.Coarse	30	1.976E-03	-
2.Medium	42	2.039E-03	3.17
3.Fine	60	2.101E-03	3.06
4.Finest	85	2.133E-03	1.51

Further validation and verification are shown in the Table 3. The designations are as described in the ITTC Quality Procedure and as follows:  $R_G$ —convergence ratio,  $p_G$ —order of accuracy,  $C_G$ —correction factor,  $U_G$ —grid uncertainty,  $\delta_{*G}$ —estimated error,  $U_{GC}$ —corrected grid uncertainty,  $S_C$ —corrected simulation value.  $U_G$ ,  $\delta_{*G}$  and  $U_{GC}$  are given as a % of the mesh independent total resistance coefficient value. From the results it is possible to see that monotonic convergence was achieved ( $0 < R_G < 1$ ) with an order of accuracy of 1.96, that is less than the estimated order of accuracy of 2. The correction factor  $C_G$  is approximately 1 and therefore resulting in a high confidence (ITTC, 2017).

Table 3 Uncertainty analysis for simulations with the device

Simulation Name	$R_G$	$P_G$	$C_G$	$U_G\%$	$\delta_{*G}\%$	$U_{GC}\%$	$S_C$
DES	0.49	1.96	0.97	-1.51	-1.5	0.0	2.16E-03

Accurate prediction of torque and thrust is dependent on the wake field and the self-propelled setup was able to successfully predict the produced torque with less than a 2% deviation from the sea trials measurements (Pena et al, 2019). On the other hand, the uncertainty analysis of the set-up with the

device showed high confidence. Therefore, the numerical setup is deemed validated and verified for further analysis.

#### 4.6. Effects of the Tubercled ESD on the Ship Efficiency

Predictions of the total resistance for the cases with and without the device are shown in the Fig. 13. As can be seen, the relative changes in the total ship resistance due to the installation of the tubercled ESD are significant. On average, the addition of the tubercled ESD provided with a 6% of reduction in the resistance of the hull. This is mainly due to the reduction in the viscous drag caused by the mixing of the boundary layer. The biggest increase is seen at the higher ship speed. This is expected as the intensity of the created mixing vortices is directly proportional to the flow velocity that reaches the tubercled ESD.

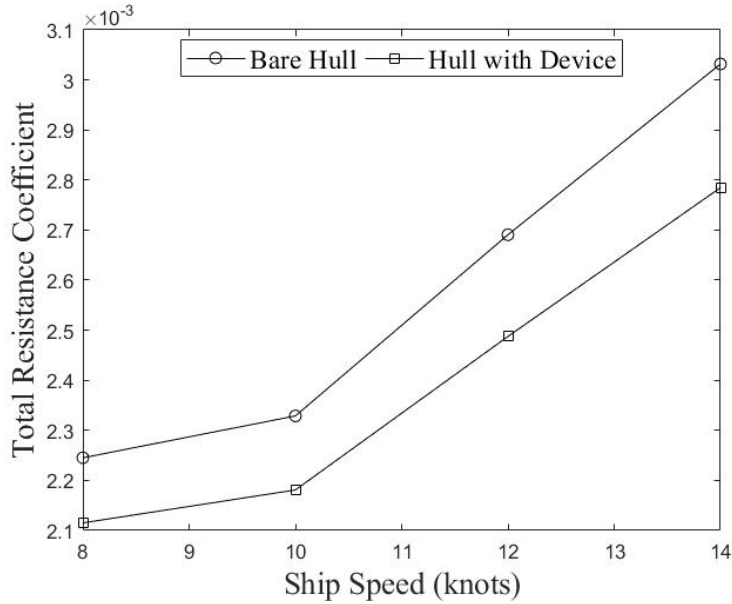


Fig. 13. Total resistance coefficient with and without device at three different shaft speeds

Nominal wake axial velocity plots at the propeller disc are presented in the Fig. 14. The figure is showing non-dimensional x-velocity contours ( $U_x/U_\infty$ ). Red/orange regions indicate the existence of slow fluid whereas blue indicates a flow speed close to the main freestream.

For the bare hull case it is identified that intense hook-shape flow pattern located at approximately 5 o'clock and the 7 o'clock positions. This hook-shape is caused by a strong bilge vortex that typically forms behind full block coefficient ships. In addition, the image depicts the existence of a reversed flow upstream of the propeller (red areas). Significant differences in the measured axial velocity indicates that the vessel may be suffering from blade load fluctuations and possible vibrations. On the other hand, the velocity field shows that the separated areas on the propeller plane occupy a big extent of the region, therefore causing potential detriment on the propeller's performance and the total ship resistance. While these nominal observations are significant, the total penalty on the propeller performance should be studied once the propeller is in place.

For the hull with the device a clear reduction of the bilge vortex detrimental effects is identified. In general, the nominal wake field seems more homogeneous and it presents higher velocities across the entire disc. At 5 o'clock and the 7 o'clock positions an increase in the axial velocity of approximately a 44% is seen. At 0.7R and approximately 3 o'clock and 9 o'clock positions, close to free-stream velocity islands are identified. This is expected due to mixing in between higher and lower momentum regions of the ship boundary layer.

As a drawback, at the edge of the nominal wake field, and the region in between 4 to 8 o'clock, a reduction in the axial velocity is seen. This is logic as the flow close to the inviscid flow region has been dragged to the inner regions of the boundary layer.

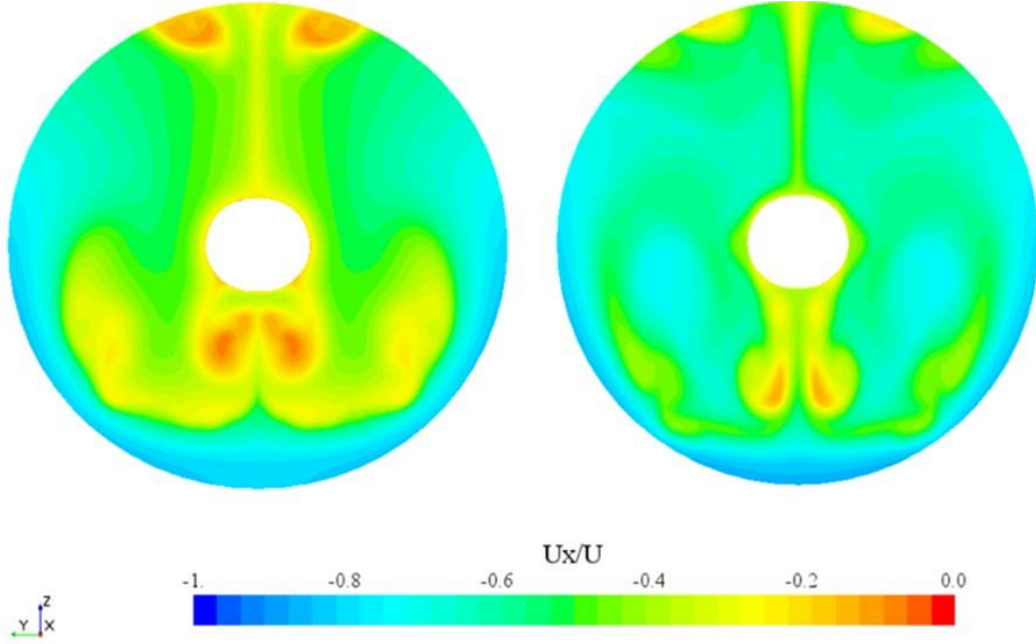


Fig. 14. Mean nominal wake field with (right) and without device (left)

Nevertheless, the nominal wake field has improved, reducing the probability of blade load fluctuations occurrence. This improvement is demonstrated by comparison of Taylor's mean nominal wake fraction of the hull with and without the novel ESD. The mean wake fraction,  $\overline{w}_n$ , across the propeller disc is found by integrating the wake field in the following form (Carlton, 2012):

$$\overline{w}_n = \frac{\int_{r_h}^R r \int_0^{2\pi} w_{n_i}(\varphi, r) d\varphi dr}{\pi(R^2 - r_h^2)} \quad (1)$$

$$w_{n_i} = \frac{\overline{U_\infty - u_{x_i}}}{U_\infty} \quad (2)$$

where  $r_h$  is the hub's radius,  $\varphi$  is the angle of rotation in propeller's plane and R is the propeller radius.

Calculated  $\overline{w}_n$  for the hull with and without device is shown on the table XX.  
**TABLE SHOWING MEAN WAKE FRACTIONS WIL BE PASTED SOON**

In general, the attached tubercled ESD can be considered as a promising energy saving technology. On the one hand, successful retrofit of the device onto a general cargo ship has revealed a reduction in the resistance of approximately a 6%. In addition, the device has shown to achieve a considerable wake improvement by swirling the flow, redistributing the momentum across the boundary layer and making the propeller loading more homogeneous. This is expected to enhance the propeller's performance.

## 5. Discussion and Conclusions

This paper has focused on the conception of a novel energy saving device based on an ancient biomimetic technology called 'tubercles'. The novel ESD is created with the aim of controlling and manipulating the flow around the hull as desired. This is the first time that tubercles are applied onto an ESD solution for ships.

Based on the mechanisms of action found in turbulent flow regime together with the analysis of the flow around the ship it was possible to design a novel biomimetic energy saving technology. This ESD achieves the desired energy saving effect for purpose.

First tests conducted showed that the attached tubercled ESD can be considered as a promising energy saving technology. On the one hand, successful retrofit of the device onto a general cargo ship has shown a reduction in the resistance of approximately a 6%. In addition, the device was able to achieve a considerable nominal wake field improvement. This was done by swirling the flow, redistributing the momentum across the boundary layer and making the propeller loading more homogeneous.

More tests are required to confirm the benefit of this novel ESD. First the authors will conduct self-propulsion tests and confirm the total energy saving before optimizing the novel ESD concept. Finally, experimental tests would be beneficial.

## References

- Carlton, J. (2012). *Marine Propellers and Propulsion*.  
<https://doi.org/10.1016/B978-0-08-097123-0.01001-7>
- Corsini, A., Delibra, G., & Sheard, A. G. (2013). On the role of leading-edge bumps in the control of stall onset in axial fan blades. *Journal of Fluids Engineering-Transactions of the Asme*, 135(8), 81104. [https://doi.org/Artn 081104rDoi 10.1115/1.4024115](https://doi.org/Artn%20081104rDoi%2010.1115/1.4024115)
- DNV GL. (2016). Propulsion Improving Devices. Retrieved from <http://glomeep.imo.org/technology/propulsion-improving-devices-pids/>
- Fish, F. E., & Battle, J. M. (1995). Hydrodynamic design of the humpback whale flipper. *Journal of Morphology*, 225(1), 51–60. <https://doi.org/10.1002/jmor.1052250105>
- Fish, F., & Lauder, G. V. (2006). Passive and Active Flow Control By Swimming Fishes and Mammals. *Annual Review of Fluid Mechanics*, 38(1), 193–224. <https://doi.org/10.1146/annurev.fluid.38.050304.092201>
- Gougoulidis, G., & Vasileiadis, N. (2010). An Overview of Hydrodynamic Energy Efficiency Improvement Measures (pp. 1–11).
- Hemmera Envirochem Inc. (2016). Vessel Quieting Desing, Technology, and Maintenance Options for Potential Inclusion in EcoAction Program Enhancing Cetacean Habitat and Observation Program, (January).
- Hochkirch, K., & Mallol, B. (2000). On the Importance of Full-Scale CFD Simulations for Ships. *Numeca*, 85–95. Retrieved from [http://www.numeca-jp.com/news/images/2013\\_-\\_On\\_the\\_Importance\\_of\\_Full-Scale\\_CFD\\_Simulations\\_for\\_Ships\\_-\\_COMPIT\\_cortona.pdf](http://www.numeca-jp.com/news/images/2013_-_On_the_Importance_of_Full-Scale_CFD_Simulations_for_Ships_-_COMPIT_cortona.pdf)
- ITTC. (2017). ITTC – Recommended Procedures and Guidelines ITTC Quality System Manual Recommended Procedures and Guidelines Guideline for Model Tests of Multi-Bodies in Close Proximity ITTC – Recommended Procedures and Guidelines, 5–7.
- Johari, H., Henoch, C., Custodio, D., & Levshin, A. (2007). Effects of leading-edge protuberances on airfoil performance. *Aiaa Journal*, 45(11), 2634–2642. [https://doi.org/Doi 10.2514/1.28497](https://doi.org/Doi%2010.2514/1.28497)
- Miklosovic, D. S., Murray, M. M., & Howle, L. E. (2007). Experimental evaluation of sinusoidal leading edges. *Journal of Aircraft*, 44(4), 1404–1407. <https://doi.org/10.2514/1.30303>
- Miklosovic, D. S., Murray, M. M., Howle, L. E., & Fish, F. E. (2004). Leading-edge tubercles delay stall on humpback whale (*Megaptera novaeangliae*) flippers. *Physics of Fluids*, 16(5). <https://doi.org/10.1063/1.1688341>
- Pena, B., Muk-Pavic E., P. D. (2019). ACHIEVING A HIGH ACCURACY NUMERICAL SIMULATIONS OF THE FLOW AROUND A FULL SCALE SHIP. In *ASME 2019 38th International Conference on Ocean, Offshore and Arctic Engineering*.
- Ponkratov. (2016). Workshop on Ship Scale Hydrodynamic Computer Simulation, (Lloyd’s Register).
- Rostamzadeh, N., Hansen, K. L., Kelso, R. M., & Dally, B. B. (2014). The formation mechanism and impact of streamwise vortices on NACA 0021 airfoil’s performance with undulating leading edge modification. *Physics of Fluids*, 26(10), 1–22. <https://doi.org/10.1063/1.4896748>
- Rostamzadeh, N., Kelso, R. M., & Dally, B. (2017). A numerical investigation into the effects of Reynolds number on the flow mechanism induced by a tubercled leading edge. *Theoretical and Computational Fluid Dynamics*, 31(1). <https://doi.org/10.1007/s00162-016-0393-x>
- Shi, W., Rosli, R., Atlar, M., Norman, R., Wang, D., & Yang, W. (2016). Hydrodynamic performance evaluation of a tidal turbine with leading-edge tubercles. *Ocean Engineering*, 117(November), 246–253. <https://doi.org/10.1016/j.oceaneng.2016.03.044>
- Skillen, A., Revell, A., Pinelli, A., Piomelli, U., Favier, J. (2014). Flow over a wing with leading-edge undulations.
- Skillen et al. (2015). Flow over a Wing with Leading-Edge Undulations. *AIAA Journal*, 53(2), 464–472. <https://doi.org/10.2514/1.J053142>
- Swanson, T., & Isaac, K. M. (2011). Biologically Inspired Wing Leading Edge for Enhanced Wind Turbine and Aircraft Performance. *Proceedings of the 6th AIAA Theoretical Fluid Mechanics Conference June 27 - 30, 2011, Honolulu, Hawaii*, 3533–3542. <https://doi.org/doi:10.2514/6.2011-3533>

- Watts, P., & Fish, F. E. (2001). The influence of passive, leading edge tubercles on wing performance. *Proc. Twelfth Intl. Symp. Unmanned Untethered Submers. Technol., Durham New Hampshire*, 2–9. Retrieved from [http://www.otherpower.com/images/scimages/2637/leading\\_edge\\_tubercles.pdf](http://www.otherpower.com/images/scimages/2637/leading_edge_tubercles.pdf)
- Weichao Shi, Mehmet Atlar, Rosemary Norman, & Kwang-cheol Seo. (2014). CFD investigations on leading-edge tubercles as applied on a tidal turbine blade. *Grand Renewable Energy 2014, P-Oc-1-12*(November).